STUDY OF BEHAVIOUR OF SOLAR THERMAL STORAGE WITH MAGNETIZED NANOFLUIDS

SAMI, S.

Faculty of Engineering, University of North Dakota, North Dakota, United State of America.
e-mail: dr.ssami[at]transpacenergy.com

(Received 15th September 2023; accepted 20th November 2023)

Abstract. A numerical simulation model that was established after the mass and energy conservation equations coupled with the heat transfer equations and thermophysical properties of magnetized nanofluids Al2O3, CuO, Fe304, and SiO2, to predict the behavior of different phase change materials, paraffin under the effect of different operating conditions It has been observed during the phase charging process that the nanofluid Al2O3 used as heat transfer fluid exhibited the longest time compared to other nanofluids and water as base fluid. Also, the results indicated that the nanofluid Fe304 had the shortest time consumed during the phase charging process under different solar radiations. Besides, it was found the higher the nanofluid concentration the longer the time to reach a liquid fraction compared to water as a base fluid, and less thermal load is needed to reach the threshold of phase change. Finally, the presented numerical model compared fairly with published experimental data under different conditions.
Keywords: *PV-Thermal, thermal storage, phase change materials, Magnetized Nanofluids, numerical modeling, model validation*

Introduction

The key factors to viable solar thermal energy storage (TES) are Phase change materials (PCMs) and Heat Transfer Fluid (HTF) (Tian and Zhao, 2013) through Gopalakrishnan et al. (2017). Phase Change Materials (PCMs) can absorb and release a large amount of thermal energy as latent heat during the phase change at a reversible quasi-isothermal process. Paraffin as a PCM is widely used as a thermal storage material due to its availability and performance at large temperature ranges (Navarrete et al., 2019; Sami and Copado, 2016; Sami and Zatarain, 2016; Sami and Tardy, 2015; Khot, 2014; Thaib et al., 2014; Tian and Zhao, 2013; Thirugnanam and Marimuthu, 2013; Ukrainczyk et al., 2010; Tardy and Sami, 2008; Elawadhi, 2005; Farid et al., 2004). Nanofluids and magnetized nanofluids exhibit superior heat transfer characteristics to conventional heat transfer fluids such as water. One of the main reasons is that the thermal conductivity of nanofluids increases significantly by the suspended particles (Xu et al., 2020; Al-Musawi et al., 2019; Al-Waeli et al., 2019; Ling et al., 2019; Sami and Marin, 2019; Sidik et al., 2019; Xu et al., 2019a, 2019b; Zhang et al., 2019; Sami, 2018; Addad et al., 2017; Gopalakrishnan et al., 2017; Sharma et al., 2017; Noro et al., 2016; Wang et al., 2014; Pise et al., 2013; Kumaresan et al., 2012; Navarrete et al., 2012; Fargali et al., 2008). The thermal conductivity of magnetized nanofluid is strongly dependent on the nanoparticle volume fraction, thus, Enhancing the thermal energy storage process. Very recently, Nuria et al. (2019) reported on “the thermal energy storage of solar salt (60% NaNO3-40% KNO3) that was improved by adding a phase change material composed of Al-Cu alloy nano capsulated with an aluminum oxide layer. He demonstrated that the total thermal energy storage was enhanced. The thermal conductivity of the nanofluid was increased when adding the nanoparticles improving its heat transfer performance”.

A novel class of nanofluid phase change materials (NFPCMs) has been presented by Kumaresan et al. (2012), "on dispersing multiwalled carbon nanotubes (MWCNTs) in water with sodium dodecyl benzene sulfonate (SDBS) as the surfactant with different volume fractions. Their work showed that an enhancement in thermal conductivity increased with MWCNT concentration and a reduction in supercooling with the addition of MWCNTs in water". Sidik et al. (2019) presented "a complete review paper, on recent progress work on cold thermal storage, PCM-CTES, and numerical and experimental studies on the heat transfer performance of different base fluids of PCMs. The work of Azwadi et al. also discussed the different factors affecting the thermophysical properties of PCMs, such as nanoparticles enhanced PCMs, the shape of encapsulated PCM volume fraction, and particle size". "The effects of pure water, SiO2/water nanofluid, and a phase-change material (PCM) as coolants on the performance of a photovoltaic thermal (PVT) system are numerically investigated. The simulations are performed on two modules of PVT with PCM (PVT/PCM module) and without (PVT module). Parameters including PV surface temperature, thermal, and electrical efficiencies of the systems are studied and compared with each other. Moreover, the results of nanofluid as a working fluid are compared with those obtained using pure water. The results show that in the water-based PVT/PCM, the average PV cell temperature is decreased compared to that of the PVT system. This results in an increase in the electrical efficiency and the thermal efficiency. In addition, using nanofluid (SiO2) as a coolant in the PVT/PCM system increases the thermal efficiency compared to that of the PVT/PCM with pure water as a coolant. This study shows that increasing the melting temperature of the phase-change material leads to an increase in the thermal efficiency of the PVT/PCM system".

The modeling of nanophenomena (Al-Musawi et al., 2019) has been presented and used "the Heat Balance Integral Method (HBIM), as an approximate solution analytical method. The author discussed the analysis of the boundary layer flow of a nanofluid and showed that Brownian motion, thermophoresis of heat transfer mechanisms and heat transfer decrease with nanoparticle concentration, which is contrary to the results that have been reported in the literature". The review paper (Gopalakrishnan et al., 2017) presented and provided "an overall of the types of thermal energy storage systems, enhancement techniques of thermal conductivity, and a general assessment of the TES. It also discussed the main challenges for the use of nanofluids in TES, the Brownian motion of nanoparticles, and the stability of nanofluids". Added et al. (2017) studied "the thermal effects of using nanofluid as a heat transfer fluid (HTF) in a thermocline-type packed-bed energy storage tank filled with spherical phase-changing material (PCM) capsules. Fortran code has been developed and validated using existing experimental and numerical data. His work showed that the use of a nanofluid as HTF was able to accelerate the charging and discharging periods, and positively impacted the thermal storage efficiency".

A paper presented by Pise et al. (2013), to "study the enhancement of the performance of paraffin wax with nano alumina (Al2O3) particles in different mass fractions, Thermal Energy Storage (TES) System at a constant flow rate and variable temperature of heat transfer fluid (HTF). Addad et al. (2017) studied the effect of alumina nanoparticles on the total cyclic time of TES for a different mass fraction. Commercially available paraffin wax was used as a phase change material (PCM). The results illustrated that the suspended nanoparticles substantially increased the heat transfer rate and also the nanofluid heat transfer rate was increased at higher

nanoparticles mass fractions". Sami and Marin (2019) recently developed "a simulation model to predict the behavior of a hybrid system composed of a PV-Thermal panel and thermoelectric generator using nanofluids; Al2O3, CuO, Fe3O4, and SiO2. The model has been based upon the energy and mass conservation equations for nanofluid flow, the dynamic behavior of the PV-Thermal solar panels, and the thermoelectric generator. The model prediction is fairly compared with existing data. Xu et al. (2019c; 2015) as well as Xu and Xing (2017) presented significant results on PCM with and without a porous medium to show the solid-liquid interface of pure PCM in the line area and the mushy area. Their findings showed that the heat transfer by natural convection in the melting liquid was significant for a PCM without a porous medium. They have also reported that the porous medium weakened the heat transfer by natural convection, however, it made the profile of the temperature field, flow field, and solid-liquid interface distribution more homogeneous. They also concluded that the metal foam can greatly improve the heat storage process and the rate of a PCM".

Our study is intended to present and investigate the phase change material and the thermal storage process driven by a PV-Thermal solar hybrid system using magnetized nanofluids under different conditions including solar radiations. In the following, we present a mathematical formulation for predicting the behavior of the thermal storage process using phase change material (PCM) and magnetized nanofluids as the heat transfer fluid in an integrated PV-thermal solar panel loop. The model was established after the energy conservation coupled with the heat transfer equations. This model was intended to study the effect of different operating conditions such as solar radiation, different magnetized nanofluids as working fluids, flow rates, nanofluids, and paraffin wax temperatures on the thermal storage process and system performance as well as the thermal energy conversion efficiency. The practical application of this study is enhancing the heat transfer process and thermal storage in solar energy systems which are one of the most critical issues to achieve a better performance of these systems with compact designs and higher efficiency.

Materials and Methods

Mathematical model

As depicted in *Figure 1*, he system under question is composed of a PV-Thermal solar panel, thermal tank, paraffin wax as PCM, and nanofluids heat transfer loop. The thermal tank with paraffin had a diameter of 0.49 meters and a length of 0.90 meters. The thermal tube inside the paraffin wax had a 0.02 diameter and length of 7.6 meters. The volume of the paraffin wax was 0.0169 m3. The magnetized nanofluid heat transfer fluid (HTF) circulates in thin tubes that were welded to the backside of the PV solar panel to absorb the heat dissipated from the solar radiation energy conversion process in the PV panel. The phase change material PCM is paraffin wax. The paraffin wax was embedded in the thermal tank as shown in *Figure 1*. The proposed model was based on the following assumptions: PCM was homogeneous and isotropic, the HTF with nanofluids was incompressible and it can be considered as a Newtonian fluid, and inlet conditions were assumed constant. Initially, PCM was in the solid-state phase as well as the thermophysical properties of the HTF with magnetized nanofluids. The PCM thermophysical properties were also assumed constant during the phase change process; solid phase, muchy phase, and liquid phase.

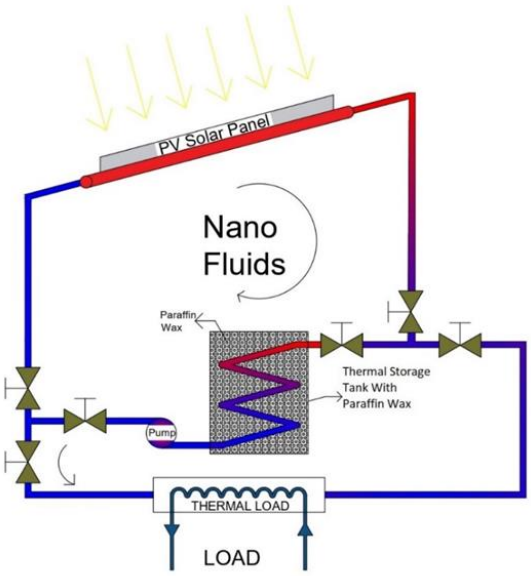

Figure 1. *Thermal storage using nanofluids.*

Solar PV model

The PV solar panels' electric circuit was composed of a load controller, batteries, and an inverter. The output voltage of the PV solar circuit was DC power and was converted into AC power using the inverter. The AC power of the inverter output P(t) of the PV solar panels was calculated using the following equation (1) with the inverter efficiency η_inv , output voltage between phases, neutral V_fn,and for single-phase current, I_o and the power factor, cosφ as follows (Eq. (1):

$$P(t) = \sqrt{3}\eta_{inv} V_{fn} I_o cos\varphi \qquad \text{Eq. (1)}$$

terested readers in the calculation of the different terms of Eq. (1) are advised to consult Pise et al. (2013), Sami and Marin (2019) as well as Sami (2018) for further details

Thermal energy incident in a PV cell

The thermal energy dissipated and transferred from the PV solar panels to the Heat Transfer Fluid (HTF) can be determined from the following heat balance in terms of heat transfer mechanisms; conduction, convection, and radiation as follows (Sami and Marin, 2019; Sami, 2018; Pise et al., 2013):

$$Q_{conduction} = Q_{convection} - Q_{radiation} \qquad \text{Eq. (2)}$$

Where, Qconduction: Thermal heat transferred by conduction; Qconvection: Thermal heat transferred by convection; and Qradiation: Thermal heat transferred by radiation. Interested readers in the calculations of the various terms in the heat balance Eq. (2) are advised to consult (Sami and Marin, 2019; Sami, 2018; Pise et al., 2013). The finite-difference formulation has been implemented to determine the HTF flow rate and its temperatures at each element. Each element was considered in the finite element analysis as a finite control volume. The thermal energy dissipated from the back of the

PV cell to the heat transfer fluid (HTF) was obtained by the following equation (Pise et al., 2013):

$$Q_{Thermal} = \dot{m}w \times C_{p\_water} \times \Delta T(T_{fHx+1} - T_{f\_In}) \quad \text{Eq. (3)}$$

Where, Q:Thermal: Heat from the thermal process; TfHx+1: Fluid temperature at thermal element (f+1); Tf-in: The fluid temperature at thermal element; and ṁw: mass flow rate of HTF.

Thermal storage and phase change material (PCM)

The phase change material experienced three phases: solid-state, liquid-state, and mushy-state. The solid and liquid phases have sensible heat additions, however, the mushy phase has latent heat addition. The heat released from the HTF to the Phase Change Material (PCM) can be written as follows (Sami and Copado, 2016; Sami and Zatarain, 2016):

$$\rho_{PCM} V_{PCM} Cp_{PCM} \frac{\Delta T_{PCM}}{\Delta t} = Qtub = m_w Cp_w \Delta T_w \quad \text{Eq. (4)}$$

Where; ΔT_w: The heat transfer fluid temperature difference; ΔT_{PCM}: The phase change material temperature difference. AndQ tub: Heat transfer per tube (kJ); and $\rho_{PCM}, V_{PCM}, Cp_{PCM}$ are the density, volume, and specific heat of the phase change material (PCM), respectively. m_w, Cp_w is the mass flow rate of the HTF water-based and the specific heat of the HTF. The heat balance for the heat exchanger tube in the thermal tank can be formulated as follows (Sami and Copado, 2016; Sami and Zatarain, 2016):

$$(T_{in} - T_{out}) Cp_w m_w = 2\pi R l h (T_{in} - T_{sfc}) \quad \text{Eq. (5)}$$

Where, h Represents the heat transfer coefficient HTF and the phase change material, and R, l is the tube radius and length of the tube, respectively. Readers interested in the calculation of the heat transfer coefficient in Eq. (5) are advised to consult (Sami and Copado, 2016; Sami and Zatarain, 2016) for further details.

Changing phase process

During the charging phase of the phase change material PCM, the HTF mass flow rate can be calculated from the thermal heat released from the PV-Thermal solar panel and absorbed by the PCM as per Eq. (4). The phase change material in the thermal tank was divided into different elements. Each element was treated as a discrete control volume. During the phase change process, phase change material experienced a phase change from liquid to mushy and solid while storing the heat absorbed during the charging process. The finite-difference formulation was used to determine the different temperatures of the phase change material as per the following equations.

Solid phase

$$T_{PCM_{m+1}} = T_{PCM_m} + \frac{m_w Cp_w \Delta T_w}{\rho_s V_{PCM} Cp_s} \Delta t \quad \text{Eq. (6)}$$

Where, T_{PCM_m}, the temperature of PCM at m element (°C). Finite difference formulation can also be applied to determine the phase change material characteristics in the mushy and liquid phases as follows.

Mushy phase

$$\gamma_{m+1} = \gamma_m + \left(\frac{m_w Cp_w \Delta T_{w,mushy}}{\rho_l V_{PCM} h_l}\right)\Delta t \qquad \text{Eq. (7)}$$

Where, γ_m, is Liquid fraction at m element (%),ΔT_w is the temperature difference in the mushy varied between 3-9 ˚C depending upon the melting point of the type of phase change materials displayed in *Table 1*. The heat transferred per tube to the phase change material is.

$$Qtub = \rho_L V_{PCM} h_L \gamma \Delta t \qquad \text{Eq. (8)}$$

Table 1. *Properties of magnetized nanofluids.*

	Ai_2O_3	CuO	Fe_3O_4	SiO_3
$C_{p\,nf}$	b = 0.1042a + 6226.5	b = 0.2011a + 5730.8	b = 0.8318a + 4269.8	b = 0.6187a + 4293.2
K_{nf}	b = 2E-05a + 1.4888	b = 5E-05a + 1.3703	b = 0.0002a + 1.0209	b = 0.0001a + 1.0265
h	b = 0.0031a + 73.092	b = 0.0031a + 73.073	b = 0.003a + 73.225	b = 0.003a + 73.231

Liquid phase

The PCM liquid temperatures can be calculated as:

$$T_{PCM_{m+1}} = T_{PCM_m} + \frac{m_w Cp_w \Delta T_w}{\rho_l V_{PCM} Cp_l}\Delta t \qquad \text{Eq. (9)}$$

Discharge phase process

During the discharge process, phase change material experienced a phase change from liquid to mushy and solid while yielding heat absorbed during the charging process. The water mass flow rate of heat transfer fluid during the discharge process can be calculated.

$$m_w = \frac{Q_{Charging}}{Cp_w \cdot \Delta T_w \cdot n} \qquad \text{Eq. (10)}$$

Therefore, the total heat absorbed $Q_{Charging}$ during the charging process, the phase change material during solid, mushy, and liquid phases can be given by:

$$Q_{Charging} = m_{PCM}(Cp_s \Delta T_s + h_L + Cp_L \Delta T_L) \cdot n \qquad \text{Eq. (11)}$$

Where, m_{PCM} is the mass of PCM per finite different element, and n is represents the number of finite different elements of the phase change material.

Nanofluid heat transfer fluid

The thermophysical, thermodynamic, and heat transfer properties of the HTF with nanoparticles can be calculated as a function of the volumetric concentration of the nanoparticles flowing in the fluid flow as follows:

$$\alpha \text{ total} = \alpha \text{ particles} + \alpha \text{ base fluid} \qquad \text{Eq. (12)}$$

Where α represents a particular thermophysical property of the nanofluid. The nanofluid thermal and thermophysical properties can be evaluated in terms of the base fluid heat transfer as follows:

$$\alpha_{total} = \alpha_{base\ fluid} + \alpha_{particles}(\Phi) \qquad \text{Eq. (13)}$$

Where Φ represents the nanoparticle's volumetric concentration. The following relationship presented in Eq. (14) was used to determine the specific heat of the nanofluids in terms of the thermal conductivity, thermal diffusivity, and density of the nanofluids as per references (Sharma et al., 2017; Pise et al., 2013; Fargali et al., 2008).

$$\lambda = \alpha\, \rho\, C_p \qquad \text{Eq. (14)}$$

Where Cp is the specific heat, α is the thermal diffusivity, ʎ and ρ represent the thermal conductivity and density, respectively. Interested readers in further details of the calculation of thermodynamic and thermophysical properties such as specific heat, density thermal diffusivity, and thermal conductivity of nanofluids are advised to consult references (Sharma et al., 2017; Xu and Xing, 2017; Wang et al., 2014; Pise et al., 2013; Fargali et al., 2008).

Magnetized nanofluids

Eq. (12) through Eq. (14) can be used to determine magnetized thermophysical properties such as α is the thermal diffusivity, ʎ, and ρ represent the thermal conductivity and density as different magnetic forces Gauss published in the literature properties (Al-Waeli et al., 2019; Sami and Marin, 2019) as a function of the Properties obtained in the *Table 1*. Where "b" represents the magnetized nanofluid-specific property and "a" is the magnetic field force in Gauss. Cpnf, Knf, and h are the specific heat, thermal conductivity, and heat transfer coefficients of the nanofluids in question.

Numerical procedure

The model presented in Eq. (1) through Eq. (14) describes the energy conversion process taking place during the charging and discharging of thermal storage in the PCM using a finite-difference element scheme as presented in *Figure 2*. The numerical calculation procedure started with the initiation of the dependent and independent parameters of solar radiation, geometrical configuration, thermodynamic and thermophysical properties of the base fluid, nanofluids, and phase change material paraffin as per *Figure 2*. This was followed by solving the mass and energy equations during charging and discharging processes written in finite-difference formulation under different boundary conditions for the base fluid water and different nanofluids under investigation. Iterations were performed using MATLAB iteration techniques until a converged solution was reached to an acceptable iteration error. Finally, the thermal energy stored in the phase change material was determined and the impact of nanofluids on the charging and discharging phase processes was also assessed.

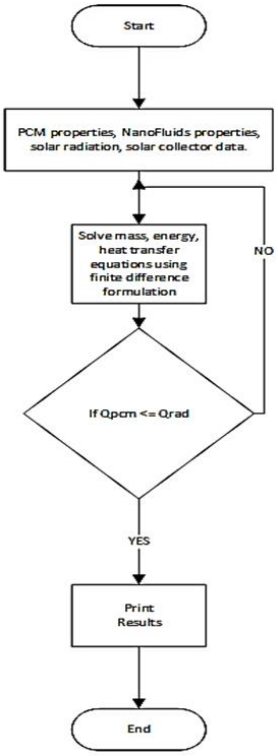

Figure 2. *Numerical procedure for finite difference scheme.*

Results and Discussion

The model presented in Eq. (1) through Eq. (14) has been numerically solved in finite-difference formulation for the energy conversion during the charging, and discharge processes of phase change materials paraffin in the hybrid system of PV-Thermal solar collector under consideration. The impact of magnetized nanofluids; AI2O3, CuO, Fe304, and SiO2 on the phase charging process of the three kinds of paraffin as per *Table 2* will be presented and discussed hereby. The different paraffin wax presented in *Table 2* was selected because of commercial availability and the availability of thermal and thermophysical properties (Sami and Copado, 2016; Sami and Zatarain, 2016). The temperature variation was taken into consideration in the calculation of the specific heat of the phase change material paraffin wax (Sami and Copado, 2016; Sami and Zatarain, 2016; Ukrainczyk et al., 2010) in the numerical simulations. In the following sections, the predicted results were presented for different types of phase change materials, paraffin; under different inlet conditions such as solar insolation, heat transfer fluid flow rates circulating from the PV-Thermal solar collector, heat transfer fluid temperatures and various magnetized nanofluids at different volumetric concentrations. In the numerical simulation, 108 PV solar panels were assumed with 120 watts per PV solar panel. Solar radiations were taken as 500 w/m2, 750 w/m2, 1000 w/m2, and finally 1200 w/m2.

Table 2*. Paraffin wax properties.*

Paraffin PCM 1		Paraffin PCM 2		Paraffin PCM 2	
Melting point	46. 7 °C	Melting point	41 °C	Melting point	37 °C
Specific heat (Solid)	2.89 kJ/kg°K	Specific heat (Solid)	2.48 kJ/kg°K	Specific heat (Solid)	1.82 kJ/kg°K

Specific heat (Liquid)	2.89 kJ/kg°K	Specific heat (Liquid)	2.76 kJ/kg°K	Specific heat (Liquid)	2.17 kJ/kg°K
Density (Solid)	947 kg/m3	Density (Solid)	29 kg/m3	Density (Solid)	911 kg/m3
Density (Liquid)	750 kg/m3	Density (Liquid)	765 kg/m3	Density (Liquid)	799 kg/m3
Latent heat	209 kJ/kg	Latent heat	288 kJ/kg	Latent heat	201 kJ/kg

A typical temporal thermal heating load during the charging process of the phase change process is presented in *Figure 3* to *Figure 5* at solar radiation of 750 W/m2 for phase change material paraffin 1, 2, and 3 using water as heat transfer fluid. Results displayed showed that the heat absorbed and transferred from the HTF changed the PCM from a solid phase to a mushy phase where finally, thermal energy was stored. This heat transfer transferred to PCM depended upon the condition of the paraffin wax initially, paraffin thermal properties, heat transfer temperature profile, heat transfer fluid thermal properties, and solar radiation. Also, it can be seen from these figures that the time needed for each phase change depended upon the type of paraffin, and its thermal properties, as well as the thermal energy, absorbed. Furthermore, the comparison presented in *Figure 4* demonstrated that paraffin 1 has a higher heat absorbed and higher thermal energy storage compared to the other kinds of paraffin under investigation. This is an important desired characteristic in the thermal energy storage process.

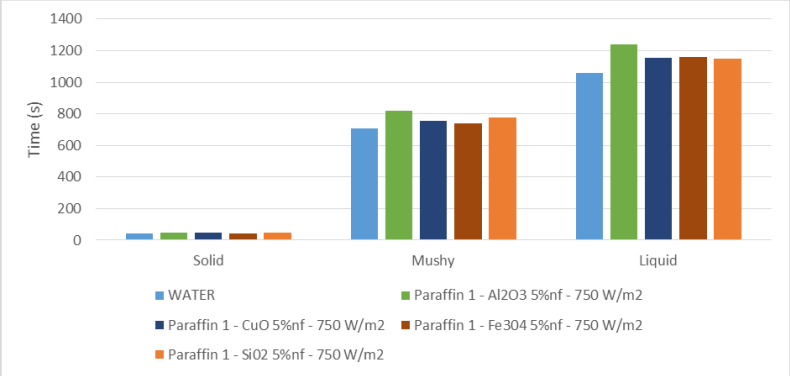

Figure 3. *Heat load during phase change process at 750W/m2.*

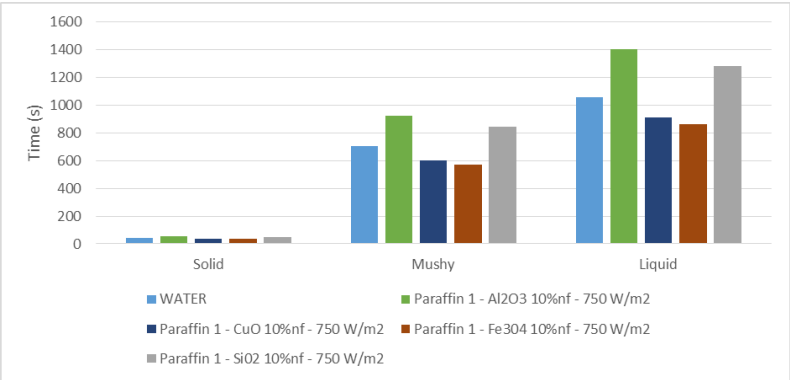

Figure 4. *Heat load during phase change process at different kinds of paraffin.*

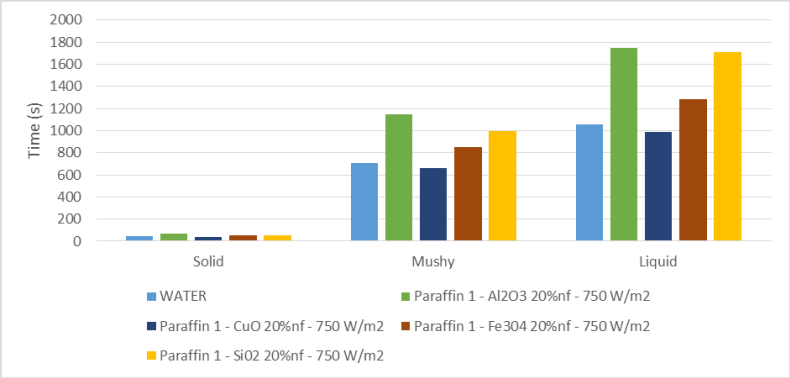

Figure 5. *Comparison of heat loads during the phase change process.*

Values displayed in *Table 1* of specific heat of and the latent heat of fusion for the different kinds of paraffin obtained from Sami and Copado (2016) as well as Sami and Zatarain (2016) were considered in the calculations. To illustrate the impact of magnetized nanofluid concentrations on thermal energy storage and phase change material process, *Figure 3* to *Figure 6* have been constructed where the charging and discharging time needed and thermal capacity of the paraffin 1, was displayed under solar radiation; 750 W/m2. Similar behavior has been observed for the other solar radiations up to 1200 W/m2. It can be seen from the results in these figures that the higher magnetized nanofluid concentrations result in high thermal storage capacity and higher thermal energy absorbed. Also, it has been observed that the higher the solar radiation the higher the thermal energy absorbed by the paraffin 1 and the higher the thermal energy storage. This can be attributed to the fact that during the melting process, the higher solar radiation absorbed by the PV solar panels resulted in higher heat transfer by convection to the heat transfer fluid circulating in the heat exchanger tubes soldered under the PV solar panels. This heat transfer by convection became very significant and resulted in an increase in heat transfer rate transferred to the PCM and caused a higher liquid fraction that accelerated the melting process from the solid phase into the latent/muchly phase to a liquid phase. It also can be observed that the charging time was gradually reduced during the phase change process because the heating continued and the molten PCM region was transformed rapidly. Most importantly, it was observed that magnetized nanofluid AI2O3 has the highest absorbent of thermal energy compared to other nanofluids under investigation. Also, the higher the concentration the higher the heat transfer absorption.

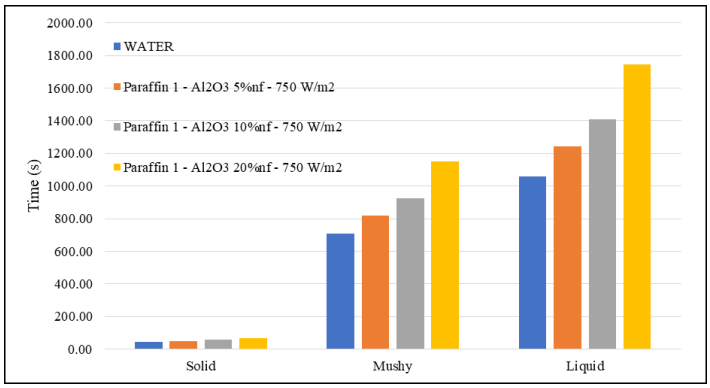

Figure 6. *Comparison of time during the phase change material process with AI2O3.*

As the nanofluid Al2O3 has the highest heat transfer absorption and is one the most studied in the literature nanofluid, *Figures 6* to *Figure 8* demonstrated that the higher volumetric concentrations of Al2O3 impacted positively the behavior of the different kinds of paraffin; 1, 2, and 3, and the phase change material process during the solid, mushy, and liquid phase change due to the resultant variation in the thermal conductivity and dynamic viscosity that were in agreement with the results reported in Ling et al. (2019) and others. As shown in *Table 1*, the phase change materials have different fusion temperatures, and their reaction to the magnetized nanofluid as heat transfer fluid during the charging process is different. Also, the Paraffin PCM-1 had the highest fusion temperature. It is also evident that augmenting the volume concentration increased the melting time of the PCMs depending upon the type of phase change material and its thermophysical properties. Thus, we clearly, state that the higher the fusion temperature the higher the charging time and the less the charging thermal load this is very beneficial since the thermal storage process can be accomplished with fewer thermal charging loads using this nanofluid. Results in *Figure 9* showed that AI2O3 has a higher performance in thermal storage, due to its higher fusion temperature. The liquid fraction profile at the different melting times for the PCM 1 was displayed in *Figure 10* to show an increased heat transfer rate to the PCM 1 with nanofluid AI2O3 at solar radiation 750 W/m2, at a higher liquid fraction accelerating the melting process of the PCM until it reached the threshold level of the liquid region as it is apparent that the higher the nanofluid concentration the longer the time to reach a liquid fraction of 100%. Therefore, less thermal load was needed to reach the threshold of the liquid phase as per *Figure 9*. Also, this figure clearly illustrated the transformation that took place from the solid to the liquid phase in the mushy region of paraffin PCM 1. Therefore, it can be concluded that more thermal energy can be stored in the phase change material with less thermal charging load using nanofluid AI2O3 compared to water as heat transfer fluid.

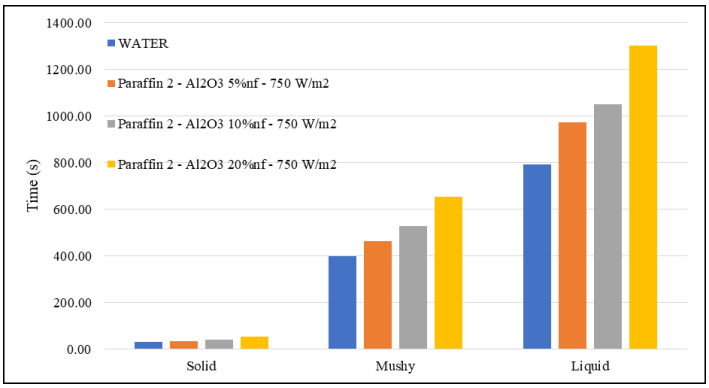

Figure 7. *Comparison of time during the phase change material process with AI2O3.*

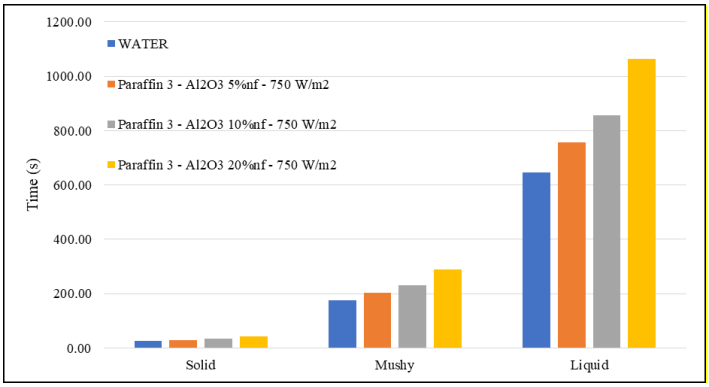

Figure 8. *Comparison of time during the phase change material process with AI2O3.*

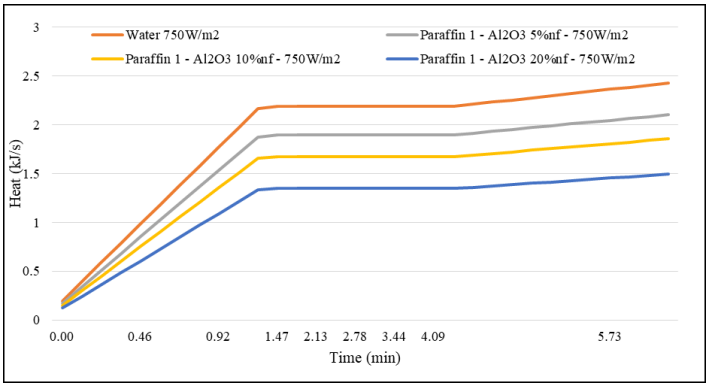

Figure 9. *Thermal load during the process of changing PCM 1 with AI2O3.*

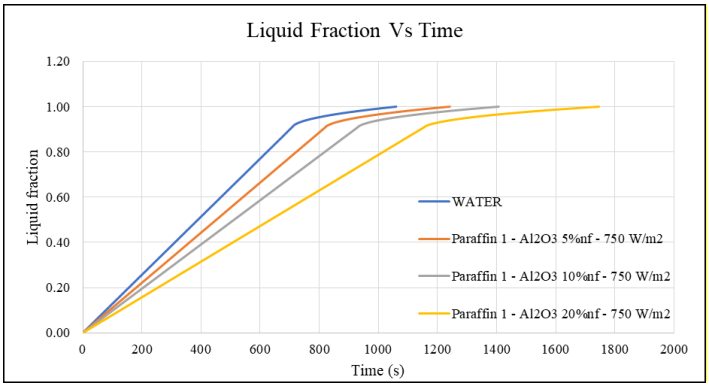

Figure 10. *The process of PCM 1 melting with AI2O3 at different concentration.*

It is quite evident from the results displayed in *Figure 10* that the higher the nanofluid concentration the lower the liquid fraction values. Also, the higher the nanofluid concentration the longer the liquid fraction takes to reach the threshold of 1.00 which represents the full transformation from the mushy phase to the liquid phase. This can be attributed to the fact that the PCM has relatively low thermal conductivity and the higher the nanofluid concentration the higher the heat transfer from the heat transfer fluid to the PCM and the longer the time it took to absorb the heat necessary for the phase change the of the paraffin. Obviously, as per *Table 1* other kind of paraffin will take a longer time to achieve the threshold of liquid phase depending upon their thermal and thermophysical properties. It is well known that the latent heat absorbed by the PCM caused it to melt during the charging process. Desirable characteristics of a solid-liquid PCM include high heat of fusion per volume, congruent melting and

freezing characteristics, high thermal conductivity, minimal supercooling, and low thermal expansion.

Figure 11 illustrates that a higher heat transfer rate was achieved at higher solar radiation with Paraffin-PCM 1. The same trend was observed for other kinds of paraffin under investigation. Moreover, *Figure 12* also showed that the lower the solar radiation the longer the time taken to achieve the change of phase during the three regions; solid, mushy, and liquid. Again, we feel the relatively low thermal conductivity of the PCM is the main reason for this observation. It is believed that improvement in the thermal storage process can be achieved by the enhancement of the thermophysical properties of the nanofluids; thermal conductivity, viscosity, and density, which are superior to those of the water. *Figures 13* to *Figures 16* illustrate the aforementioned argument with the different magnetized nanofluids under investigation: AI2O3, CuO, Fe304, and SiO2. Results using paraffin PCM 1 showed that the nanofluid Ai2O3 as heat transfer fluid exhibited the longest time compared to the other nanofluids during the three regions solid, mushy, and liquid. Also, these figures indicated that the nanofluid Fe304 had the shortest time consumed during the charging process. This finding is significant since we believe that using the nanofluid Fe304 can shorten the charging time required which is very beneficial to the charging process of the PCM. It is also worthwhile mentioning that similar behavior was observed with the other nanofluids PCM 2 and PCM 3 listed in *Table 1*. Similarly, *Figures 16* to *Figure 18* shows the impact of the use of the different nanofluids under investigation; AI2O3, CuO, Fe304, and SiO2 with different concentrations of 5%, 10% and 20% on the thermal heat absorbed at 750 w/m2 solar radiation. Other PCM2 and PCM 3 experienced the same behavior observed in Fe304. We believe that this was attributed to the enhanced thermophysical properties of Fe304. It is worthwhile mentioning that the nanofluids concentration of 20% was only used to demonstrate the impact of higher volumetric concentration on the heat absorbed. Thus, it is highly recommended to use nanofluid Fe304 during the charging process of the phase change material over other nanofluids including the water as heat transfer fluid

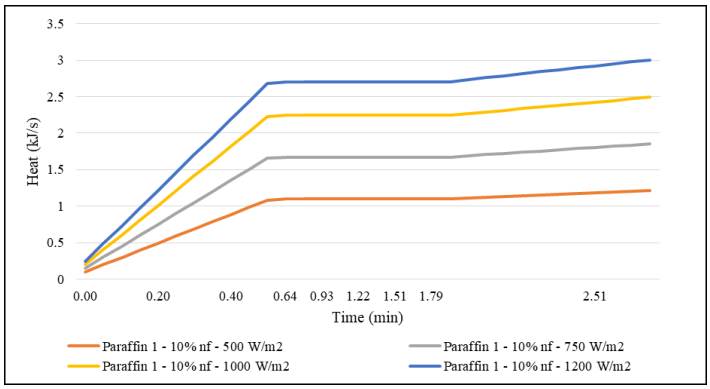

Figure 11. *The process of PCM 1 melting with AI2O3 at different solar radiations.*

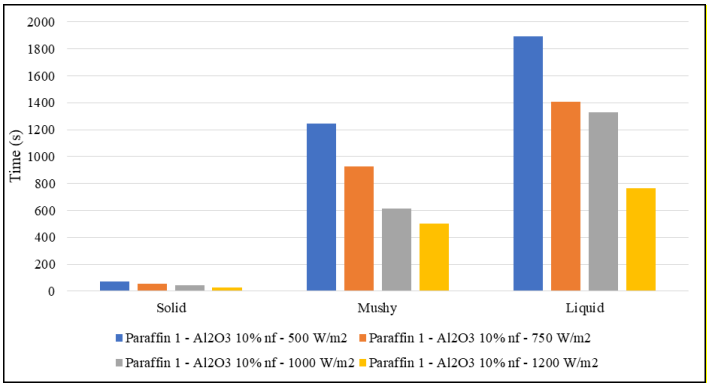

Figure 12. *The process of PCM 1 melting with AI2O3 at different solar radiations.*

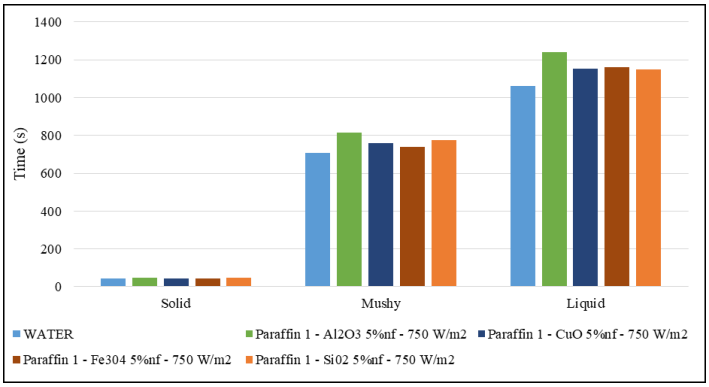

Figure 13. *The process of PCM 1 melting with different nanofluids at 5% concentration.*

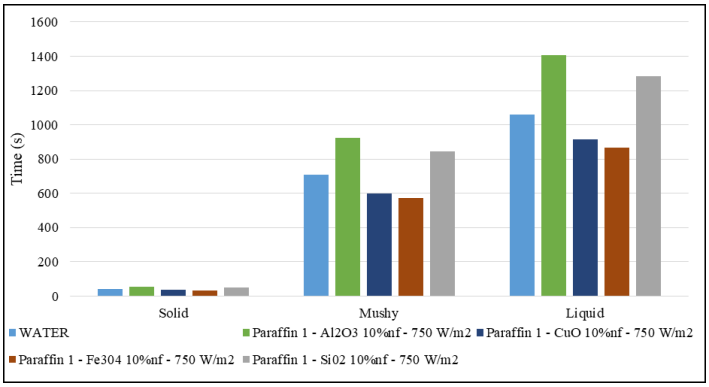

Figure 14. *The process of PCM 1 melting with different nanofluids at 10% concentration.*

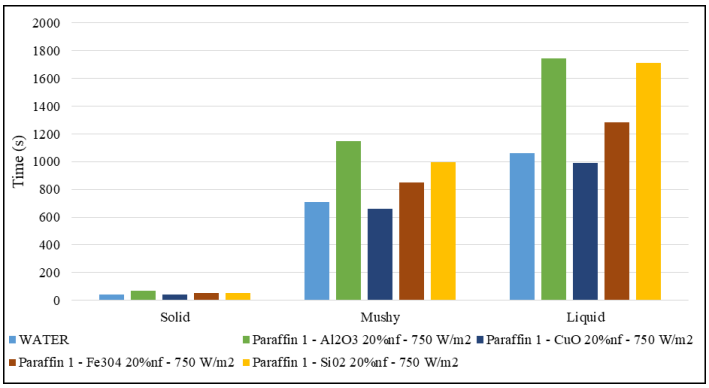

Figure 15. *The process of PCM 1 melting with different nanofluids at 20% concentration.*

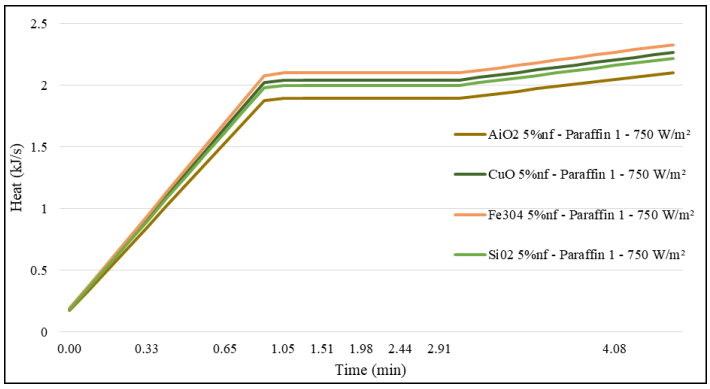

Figure 16. *The process of PCM 1 melting with different nanofluids at 5% concentrations.*

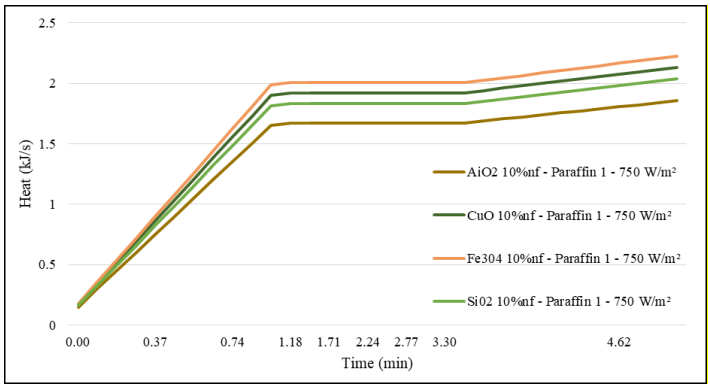

Figure 17. *The process of PCM 1 melting with different nanofluids at 10% concentration.*

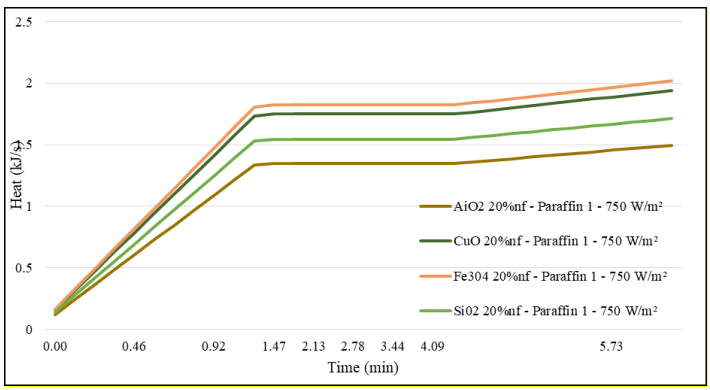

Figure 18. *The process of PCM 1 melting with different nanofluids at 20% concentration.*

Model validation

The numerical model presented hereby in Eq. (1) through Eq. (14) was validated against the experimental data reported by Abdulateef et al. (2018), during the phase change melting process using Al2O3 nanoparticles and shown in *Figure 19*. Abdulateef et al. (2018) reported that temperatures of the PCM were measured on the top and bottom of the storage tank in the axial direction. The melting point of paraffin used in Abdulateef et al. (2018) was higher than the paraffin used in this study during the sensible heating of the PCM. The comparison presented in *Figure 19* showed that there were some discrepancies between the numerical model's prediction and experimental data (Xu et al., 2015) that did not exceed 7%. This demonstrated a good agreement and

reliability of the model presented hereby. We believe that the over-prediction of the higher temperatures by our model was attributed to the over-prediction of the heat transfer coefficient and the thermophysical properties of the nanofluid Ai2O3 that resulted in higher temperatures. Furthermore, it should be noted that Abdulateef et al. (2018) did not disclose relevant information on the calculations of the heat transfer coefficient and the thermophysical properties.

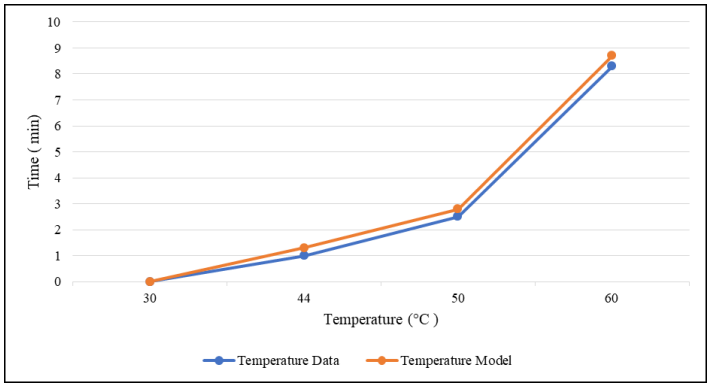

Figure 19. *Comparison between model prediction and data reference (Abdulateef et al., 2018)*

Conclusion

A mathematical model for predicting the behavior of the thermal storage process in phase change material (PCM) using magnetized nanofluids as the heat transfer fluid in an integrated PV-thermal solar panel loop with thermal storage capabilities. The model was based on energy conservation coupled with the heat transfer equations. This model studied the effect of different operating conditions such as solar radiation, working fluid flow rates, magnetized nanofluids, and paraffin temperatures and their impact on the thermal storage process, and phase change process. The results presented hereby on the use of magnetized nanofluids with PCM paraffin 1 as well as the other kinds of paraffin showed that the nanofluid AI2O3 exhibited the longest time compared to other nanofluids and water as the base fluid for charging the PCM during the three regions solid, mushy and liquid. Also, the results indicated that the nanofluid Fe304 had the shortest time consumed during the charging process. This was significant since using the nanofluid Fe304 shortened the charging time required which is very beneficial to the charging process of the PCM. It is worthwhile mentioning that similar behavior was observed with the other nanofluids with PCM 2 and PCM 3 under solar radiations; 500, 750, 1000, and 1200 w/m2. Thereafter, it was also recommended to use nanofluid Fe304 during the charging process. Finally, the model numerical prediction compared fairly with experimental data reported in the literature but showed some discrepancies that did not exceed 7%. However, it’s recommended for future studies to use more experimental studies with different kinds of paraffin wax phase change materials and different magnetized nanofluids for a broad validation of the proposed model under different conditions.

Acknowledgement

The research work presented in this paper was made possible through the support of TransPacific Energy Inc The author is indebted to all contributors for help in the computation and programming of this model.

Conflict of interest

The authors declare that there is no conflict of interest involve in this research study.

REFERENCES

[1] Abdulateef, A.M., Mat, S., Abdulateef, J., Sopian, K., Al-Abidi, A.A. (2018): Thermal performance enhancement of triplex tube latent thermal storage using fins-nano-phase change material technique. – Heat Transfer Engineering 39(12): 1067-1080.

[2] Addad, Y., Abutayeh, M., Abu-Nada, E. (2017): Effects of nanofluids on the performance of a PCM-based thermal energy storage system. – Journal of Energy Engineering 143(4): 7p.

[3] Al-Musawi, A.I.A., Taheri, A., Farzanehnia, A., Sardarabadi, M., Passandideh-Fard, M. (2019): Numerical study of the effects of nanofluids and phase-change materials in photovoltaic thermal (PVT) systems. – Journal of Thermal Analysis and Calorimetry 137: 623-636.

[4] Al-Waeli, A.H., Chaichan, M.T., Sopian, K., Kazem, H.A., Mahood, H.B., Khadom, A.A. (2019): Modeling and experimental validation of a PVT system using nanofluid coolant and nano-PCM. – Solar Energy 177: 178-191.

[5] Elawadhi, E.M. (2005): Phase change process with free convection in a circular enclosure; numerical simulation. – Computer & Fluids 33: 1335-148.

[6] Fargali, H.M., Fahmy, F.H., Hassan, M.A. (2008): A simulation model for predicting the performance of PV/wind-powered geothermal space heating system in Egypt. – The Online Journal on Electronics and Electrical Engineering (OJEEE) 2(4): 173-177.

[7] Farid, M.M., Khudhair, A.M., Razack, S.A.K., Al-Hallaj, S. (2004): A review on phase change energy storage: materials and applications. – Energy Conversion and Management 45(9-10): 1597-1615.

[8] Gopalakrishnan, G., Jabaraj, D.B., Muthuraman, V. (2017): Review on thermal energy storage system and phase change materials with dispersed nanoparticles. – Journal of Chemical and Pharmaceutical Sciences 3p.

[9] Khot, S.A. (2014): Enhancement of thermal storage system using phase change material. – Energy Procedia 54: 142-151.

[10] Kumaresan, V., Velraj, R., Nanda, M., Maini, A.K. (2012): Phase change material-based nanofluids for heat transfer enhancement in latent heat thermal energy storage system. – International Journal of Green Nanotechnology 4(4): 541-546.

[11] Ling, H., Wang, L., Chen, C., Wang, Y., Chen, H. (2019): Effect of thermophysical properties correlation of phase change material on numerical modelling of agricultural building. – Applied Thermal Engineering 157: 9p.

[12] Navarrete, N., Mondragón, R., Wen, D., Navarro, M.E., Ding, Y., Juliá, J.E. (2019): Thermal energy storage of molten salt–based nanofluid containing nano-encapsulated metal alloy phase change materials. – Energy 167: 912-920.

[13] Noro, M., Lazzarin, R., Bagarella, G. (2016): Advancements in hybrid photovoltaic-thermal systems: performance evaluations and applications. – Energy Procedia 101: 496-503.

[14] Pise, A.T., Waghmare, A.V., Talandage, V.G. (2013): Heat transfer enhancement by using nanomaterial in phase change material for latent heat thermal energy storage system. – Asian Journal of Engineering and Applied Technology 2(2): 52-57.
[15] Sami, S. (2018): Modeling and simulation of a novel combined solar photovoltaic-thermal panel and heat pump hybrid system. – Clean Technologies 1(1): 89-113.
[16] Sami, S., Copado, O. (2016): Numerical Analysis of Integrated Phase Change Material in Solar Water Heating Systems. – International Journal of Energy and Power Engineering 5: 105-112.
[17] Sami, S., Marin, E. (2019): Modelling and simulation of PV solar-thermoelectric generators using nano fluids. – International Journal of Sustainable Energy and Environmental Research 8(1): 70-99.
[18] Sami, S., Tardy, F. (2015): Numerical Prediction of Thermal Storage Using Phase Change Material. – Journal of Technology Innovations in Renewable Energy 4(3): 80-90.
[19] Sami, S., Zatarain, J. (2016): Thermal Analysis and Modelling of Thermal Storage in Solar Water Heating Systems. – International Journal of Energy and Power Engineering 5(2): 48-59.
[20] Sharma, K.V., Suleiman, A., Hassan, H.S.B., Hegde, G. (2017): Considerations on the thermophysical properties of nanofluids. – Engineering Applications of Nanotechnology: From Energy to Drug Delivery 37p.
[21] Sidik, N.A.C., Kee, C.H., Yusof, S.N.A., Mohamad, A.T. (2019): Performance enhancement of cold thermal energy storage system using nanofluid phase change materials. – Journal of Advanced Research in Applied Mechanics 62(1): 16-32.
[22] Tardy, F., Sami, S. (2008): An experimental study determining behaviour of heat pipes in thermal storage. – International Journal of Ambient Energy 29(3): 162-168.
[23] Thaib, R., Hamdani, Irwansyah, Zaini (2014): Investigation performance of solar water heater system using paraffin wax. – ARPN Journal of Engineering and Applied Sciences 9(10): 1749-1752.
[24] Thirugnanam, C., Marimuthu, P. (2013): Experimental analysis of latent heat thermal energy storage using paraffin wax as phase change material. – International Journal of Engineering and Innovative Technology 3(2): 372-376.
[25] Tian, Y., Zhao, C.Y. (2013): A review of solar collectors and thermal energy storage in solar thermal applications. – Applied Energy 104: 538-553.
[26] Ukrainczyk, N., Kurajica, S., Šipušić, J. (2010): Thermophysical comparison of five commercial paraffin waxes as latent heat storage materials. – Chemical and Biochemical Engineering Quarterly 24(2): 129-137.
[27] Wang, J., Xie, H., Guo, Z., Guan, L., Li, Y. (2014): Improved thermal properties of paraffin wax by the addition of TiO2 nanoparticles. – Applied Thermal Engineering 73(2): 1541-1547.
[28] Xu, H., Gong, L., Huang, S., Xu, M. (2015): Flow and heat transfer characteristics of nanofluid flowing through metal foams. – International Journal of Heat and Mass Transfer 83: 399-407.
[29] Xu, H., Wang, Y., Han, X. (2020): Analytical considerations of thermal storage and interface evolution of a PCM with/without porous media. – International Journal of Numerical Methods for Heat & Fluid Flow 30(1): 373-400.
[30] Xu, H., Xing, Z. (2017): The lattice Boltzmann modeling on the nanofluid natural convective transport in a cavity filled with a porous foam. – International Communications in Heat and Mass Transfer 89: 73-82.
[31] Xu, H., Xing, Z., Vafai, K. (2019a): Analytical considerations of flow/thermal coupling of nanofluids in foam metals with local thermal non-equilibrium (LTNE) phenomena and inhomogeneous nanoparticle distribution. – International Journal of Heat and Fluid Flow 77: 242-255.

[32] Xu, H., Xing, Z.B., Ghahremannezhad, A. (2019b): Lattice Boltzmann modeling on forced convective heat transfer of nanofluids in highly conductive foam metals with local thermal nonequilibrium (LTNE) effect. – Journal of Porous Media 22(12):1553-1571.
[33] Xu, H.J., Xing, Z.B., Wang, F.Q., Cheng, Z.M. (2019c): Review on heat conduction, heat convection, thermal radiation and phase change heat transfer of nanofluids in porous media: Fundamentals and applications. – Chemical Engineering Science 195: 462-483.
[34] Zhang, X., Wu, Y., Ma, C., Meng, Q., Hu, X., Yang, C. (2019): Experimental study on temperature distribution and heat losses of a molten salt heat storage tank. – Energies 12(10): 14p.